pp 489–509. © The Author(s), 2020. Published by Cambridge University Press on behalf of Royal Aeronautical Society
doi:10.1017/aer.2020.95

Estimation of aerodynamic parameters near stall using maximum likelihood and extreme learning machine-based methods

H.O. Verma and N.K. Peyada
homverma@gmail.com
homverma@aero.iitkgp.ac.in
nkpeyada@aero.iitkgp.ac.in
Department of Aerospace Engineering
Indian Institute of Technology Kharagpur
Kharagpur
West Bengal
India

ABSTRACT

The stability and control derivatives are essential parameters in the flight operation of aircraft, and their determination is a routine task using classical parameter estimation methods based on maximum likelihood and least-squares principles. At high angle-of-attack, the unsteady aerodynamics may pose difficulty in aerodynamic structure determination, hence data-driven methods based on artificial neural networks could be an alternative choice for building models to characterise the behaviour of the system based on the measured motion and control variables. This research paper investigates the feasibility of using a recurrent neural model based on an extreme learning machine network in the modelling of the aircraft dynamics in a restricted sense for identification of the aerodynamic parameters. The recurrent extreme learning machine network is combined with the Gauss–Newton method to optimise the unknowns of the postulated aerodynamic model. The efficacy of the proposed estimation algorithm is studied using real flight data from a quasi-steady stall manoeuvre. Furthermore, the estimates are validated against the parameters estimated using the maximum likelihood method. The standard deviations of the estimates demonstrate the effectiveness of the proposed algorithm. Finally, the quantities regenerated using the estimates present good agreement with their corresponding measured values, confirming that a qualitative estimation can be obtained using the proposed estimation algorithm.

Keywords: Recurrent Neural Model; Extreme Learning Machine; Parameter Estimation; Maximum Likelihood Estimation; Gauss–Newton Method; Quasi-Steady Stall Manoeuvre; Aerodynamic Model

Received 6 April 2020; revised 9 September 2020; accepted 14 September 2020.

https://doi.org/10.1017/aer.2020.95 Published online by Cambridge University Press

NOMENCLATURE

a_x, a_z	linear acceleration of aircraft along x and z axis
C_L, C_D, C_m	coefficients of lift, drag and pitching moment
$C_{L_0}, C_{D_0}, C_{m_0}$	coefficients of lift, drag and pitching moment at zero angle-of-attack
$C_{L_\alpha}, C_{m_\alpha}$	coefficients of lift and pitching moment with respect to angle-of-attack
C_{m_q}	coefficient of pitching moment with respect to normalised pitch rate
$C_{L_{\delta_e}}, C_{m_{\delta_e}}$	coefficients of lift and pitching moment with respect to elevator deflection
$\frac{\partial C_D}{\partial \chi}, \frac{\partial C_m}{\partial \chi}$	coefficients of drag and pitching moment with respect to flow separation point, χ
C_X, C_Z	body force coefficients along x and z axis
I_x, I_y, I_z	moment of inertia about x, y and z axis
I_{xz}	cross-product of inertia
n_x, n_y	number of input and output variables
n_h, n_Θ	numbers of hidden layer neurons and unknown parameters
N	number of the data samples
r_h	distance between wing and elevator
R	measurement noise covariance matrix
t	wing thickness
T	engine thrust
V	true velocity of aircraft
$\bar{V}, \bar{W}, \bar{H}$	input weight matrix, output weight matrix and hidden layer output vector
$\bar{x}_{\max}, \bar{x}_{\min}$	maximum and minimum value of specified range for normalisation of data samples
X, Y, Z	input vector, predicted output vector and measured output vector.
z_{ENCG}	vertical distance between engine location and centre of gravity of aircraft
α, θ	angle-of-attack and pitch angle
p, q, r	angular rates: roll, pitch and yaw
$\dot{\alpha}$	rate of change in angle-of-attack
a_1	static stall characteristics of aerofoil
ε	residual error
$\bar{c}$	mean aerodynamic chord
Λ	wing aspect ratio
e	oswald factor
Θ	unknown parameter vector
$\hat{\Theta}$	estimated parameter vector
χ	flow separation point
z^{-1}	time delay in data sample

Abbreviations

ANN	artificial neural network
ATTAS	advanced technology testing aircraft system

https://doi.org/10.1017/aer.2020.95 Published online by Cambridge University Press

CFD	computational fluid dynamic
CNVG	convergence
ELM	extreme learning machine
FFNN	feed-forward neural network
GN	Gauss–Newton
MLE	maximum likelihood estimation
MSE	mean square error
QSSM	quasi-steady stall manoeuvre
RELM	recurrent extreme learning machine
RFD	real flight data
RNN	recurrent neural network
STD	standard deviation
TIC	Theil's inequality coefficient

1.0 INTRODUCTION

Parameter estimation is a routine task in aircraft system identification to determine the best possible estimates of the stability and control derivatives of a postulated aerodynamic model. The derivatives are most often computed using analytical, computational and wind-tunnel methods carried out on a scaled model or prototype[1]. These approaches provide preliminary information on the aerodynamic behaviour at the initial design phase, although they may provide less accuracy due to the assumptions considered. Final verification of the aerodynamic parameters is carried out based on the results of flight testing, which is an essential step for gathering real flight data during a specific manoeuvre and computing the stability and control derivatives at higher accuracy[2,3]. Time-invariant linear aerodynamic models are preferred at low angle-of-attack[4,5], whereas unsteady aerodynamic effects are more dominant in higher angle-of-attack regimes due to the flow separation over the upper surface of the wing. Therefore, postulating an aerodynamic model is a difficult task near stall, due to the nonlinearity and cross-coupling caused by such unsteady aerodynamic effects. However, reduced-order models based on indicial functions and state-space models have been investigated to provide theoretical understanding[6–9]. The indicial functions were used to represent the transient aerodynamic response due to a step change in the angle-of-attack or pitch rate using the Duhamel superposition integral[10,11]. However, this investigation was limited to the analysis of two-dimensional aerofoils only. The analytical expressions are also found to be invalid for a complete aircraft configuration due to the effect of wing tip vortices. To handle this issue, a grid motion tool with the unsteady Reynolds-averaged Navier–Stokes simulation was applied for computational fluid dynamic (CFD)-based computations in the linear and nonlinear indicial functions with respect to the angle-of-attack and pitch rate[12]. Furthermore, a time-dependent surrogate model was also developed to compute the aerodynamic forces and moments during a flight manoeuvre through CFD simulations[13]. Leishman et al.[14] and Goman et al.[15] represented the aerodynamic forces and moments in the state-space form using the flow separation point, considered as an internal state variable for unsteady air flow. Further, the representation was employed in the postulation of an aerodynamic model for the quasi-steady stall manoeuvre using real flight data[16,17]. This incorporates additional terms due to the flow separation point in such a way as to distinguish the forces and moments for attached as well as separated flows over the main wings.

https://doi.org/10.1017/aer.2020.95 Published online by Cambridge University Press

Estimators based on maximum likelihood and least-squares principles have more often been applied in computations of aerodynamic parameters at moderate angles of attack[18,19], whereas their variants have been used to achieve better estimates in the presence of measurement and process noise[20]. Due to the increasing demand for real-time operation of aerodynamic models, recursive estimation algorithms have also been investigated using the aircraft flight data[21–23]. The lack of a priori information about the stability and control derivatives for large-amplitude manoeuvres near stall may pose a difficulty when applying classical parameter estimation methods, hence such investigations are a subject of great interest to researchers.

With the advent of data-driven tools, research has focused more on accurate aerodynamic modelling for applications such as control law design, flight simulators etc. Generally, wind-tunnel experiments are an economical approach for aerodynamic characterisation of a scaled model for the preliminary design of a prototype. Wind-tunnel data for the aerodynamic forces and moments can be mapped using a feed-forward neural network (FFNN), recurrent neural network (RNN) etc.[24,25]. Support vector machines have also been applied for nonlinear modelling of a delta-wing scaled model at high angle-of-attack[26]. A similar type of modelling was also investigated with real flight data using the decision tree and forest method by Kumar et al.[27]. Linse et al.[28] introduced an approach for estimating the stability and control derivatives from FFNN models while training the network. Raol et al.[29] introduced aerodynamic modelling using a RNN to estimate the aircraft parameters from real flight data. However, those authors pointed out the limited applications of RNN in the field of aircraft identification and parameter estimation. The input variables associated with the stability and control derivatives of the postulated aerodynamic model were also estimated using numerical methods applied on the trained FFNN[30,31]. However, these estimation approaches did not contribute to the computation of the stall parameters. Sinha et al.[32] applied the neural partial differential method in the computation of the lift curve slope from aerodynamic lift force data for single and cascaded fins of aerofoils and rectangular cross-sections using a trained FFNN. A combination of an optimisation algorithm with FFNN was also applied to compute the aerodynamic parameters from flight data gathered in moderate and high angle-of-attack regimes[33–36]. An intelligent algorithm based on the combination of neuro fuzzy and artificial bee colony methods has also been investigated in the field of parameter estimation[37]. However, the performance of these approaches is limited by the generalisation ability of the network, the training algorithms and the computational cost, which are often exacerbated by the selection of improper network parameters. A variant of FFNN, namely the extreme learning machine (ELM), which was suggested by Huang et al.[38–40], can overcome the issues of generalisation as well as the computational cost of conventional FFNN. Due to the simplicity of operation of the ELM network, various real-world problems have been solved by training the network analytically for optimally chosen input parameters[43,44].

In the current research paper, an investigation of the aerodynamic parameters is carried out using a proposed estimation algorithm based on a recurrent ELM (RELM) network. The methodology utilises the features of the ELM network in the recurrent neural modelling of the flight dynamics in a restricted sense for the parameter estimation application only. The generalisation capability of the dynamic network is evaluated in terms of the statistical values obtained for the coefficient of determination, R^2, and mean square error (MSE). Furthermore, the RELM network is combined with the Gauss–Newton (GN) method to optimise the aerodynamic parameters from real flight data (RFD) gathered from the Advanced Technology Testing Aircraft System (ATTAS) aircraft during a quasi-steady stall manoeuvre (QSSM) consisting of stall and post-stall regimes. The proposed parameter estimation algorithm is

https://doi.org/10.1017/aer.2020.95 Published online by Cambridge University Press

applied to the flight data to investigate the parameters of the nonlinear aerodynamic model. Furthermore, the aerodynamic estimates are validated using the estimates of the maximum likelihood estimation (MLE) method and their corresponding standard deviations. The simulated responses demonstrate the efficacy of the proposed parameter estimation algorithm in the presence of noise. The remainder of this manuscript is organised as follows: The next section briefly addresses aerodynamic modelling in the state-space form, then the subsequent section describes the parameter estimation methods used in the present analysis. The results and discussion section then presents the efficacy of the proposed algorithm for the extraction of the aerodynamic parameters from real flight data. Finally, important remarks based on the computation of the aerodynamic parameters are highlighted in the conclusion section, along with the pros and cons of the neural modelling and parameter estimation algorithm.

2.0 AERODYNAMIC MODEL OF QUASI-STEADY STALL

Generally, the dynamic equations of an aircraft are represented by Euler's equations of motion governed by the external forces and moments due to the aerodynamic, thrust and gravity effects. The external forces and moments due to the aerodynamic effects constitute an aerodynamic model and are defined in their respective coefficient forms at each of the operating conditions[4,5]. They are also represented using a nonlinear function of the motion and control variables as follows:

$$C_X = f(x, u) \qquad \ldots (1)$$

where C_X denote the coefficients of aerodynamic force or moment, and $f(\bullet)$ denotes the functional relationship with the flight motion and control variables.

In the postulation of an aerodynamic model, the above nonlinear function is expanded by applying a Taylor's series with the consideration of effective variables only. A linear relationship is commonly used to demonstrate the longitudinal and lateral directional motion in a decoupled way at low angle-of-attack. Due to the dominance of the unsteady aerodynamic effects, nonlinear aerodynamic models are employed in higher angle-of-attack regimes, being obtained in the form of higher degrees of motion and control variables or a model based on Kirchhoff's theory of flow separation. Near stall, the flow separation will reduce the value of C_{L_α} before the $C_{L_{MAX}}$ point and a loss of C_L is seen beyond the $C_{L_{MAX}}$ point. The trailing edge of the flow separation is a typical way of demonstrating the separation phenomenon for most conventional aircraft. Such unsteady aerodynamic effects have primarily been investigated using semi-empirical methods, computational fluid dynamic methods and wind-tunnel testing methods. Analytical approaches for these complex phenomena are primarily carried out using the indicial function, although its formulation for parameter estimation applications is difficult. Therefore, an alternative approach is adopted to describe the flow separation analytically, then further to postulate the aerodynamic model as an internal state variable. Thus, the aerodynamic model retains the conventional state-space form, and the aircraft identification and parameter estimation procedures can be applied directly on flight data.

Trailing-edge stall is a kind of stall phenomenon commonly considered on wings having thickness (t) to chord ratio ($\bar{c}$) greater than 0.15 and undergoing a slow variation in angle-of-attack (i.e. $\dot{\alpha} < 0.02V/\bar{c}$). The flow separation point is represented by a nondimensional variable, say χ, whose value varies between 1 and 0 along the chord line for the fully attached and separated flow over the upper surface of the wing, respectively. The flow separation point is theoretically formulated by using a single-order differential equation as follows[16,17]:

https://doi.org/10.1017/aer.2020.95 Published online by Cambridge University Press

$$\tau_1 \frac{d\chi}{dt} + \chi = \frac{1}{2}\left\{1 - \tanh\left[a_1(\alpha - \tau_2\dot{\alpha} - \alpha^*)\right]\right\} \quad \ldots(2)$$

where τ_1, τ_2 denote time constants corresponding to the transient and quasi-steady aerodynamic effects, respectively; a_1 denotes the static stall characteristics of the aerofoils; α^* denotes the break point of α. There are four parameters, namely $a_1, \alpha^*, \tau_1, \tau_2$, in this equation (2) that have to be estimated using real flight data. The computation of both time constants is crucial and can only be achieved from highly dynamic stall manoeuvres. Such manoeuvres are difficult and risky to execute in real flight experiments, hence the quasi-steady stall manoeuvre is most commonly used for such analysis and to postulate the aerodynamic model near stall. This can lead to an estimation of the time constant based on the quasi-steady aerodynamic effects, only. Therefore, the transient effect can be neglected by assuming that $\tau_1 = 0$, and the flow separation point, χ can be represented using the equation

$$\chi = \frac{1}{2}\left\{1 - \tanh\left[a_1(\alpha - \tau_2\dot{\alpha} - \alpha^*)\right]\right\} \quad \ldots(3)$$

Thus, three parameters, namely a_1, τ_2, α^*, are sufficient to describe the stall hysteresis, and the intermediate variable, χ, can be used in the postulation of the aerodynamic model as follows[2] :

$$\begin{aligned} C_L &= C_{L_0} + C_{L_\alpha}\left\{\frac{1+\sqrt{\chi}}{2}\right\}^2 \alpha \\ C_D &= C_{D_0} + \frac{1}{e\pi\Lambda}{C_L}^2 + \frac{\partial C_D}{\partial \chi}(1-\chi) \\ C_m &= C_{m_0} + C_{m_\alpha}\alpha + C_{m_q}\frac{q\bar{c}}{2V} + C_{m_{\delta e}}\delta_e + \frac{\partial C_m}{\partial \chi}(1-\chi) \end{aligned} \quad \ldots(4)$$

where $\frac{\partial C_D}{\partial \chi}$, $\frac{\partial C_m}{\partial \chi}$ are the derivatives of the drag force and pitching moment with respect to χ, respectively.

3.0 PARAMETER ESTIMATION METHODS

The present section demonstrates the maximum likelihood-based estimation and the proposed recurrent ELM-GN algorithm for the computation of the parameters of the QSSM. In the validation of the aerodynamic model, Theil's inequality coefficient is briefly presented to illustrate the efficacy of the proposed algorithm.

3.1 Maximum likelihood estimation

A cost function, J, is defined to optimise the parameters using the maximum likelihood function for unknown parameter vector, Θ, and the measurement noise covariance matrix, R, as follows[2,45,46]:

$$J(\Theta, R) = \frac{1}{2}\sum_{i=1}^{N} {E_i}^T R^{-1} E_i + \frac{N}{2}\ln\{\det(R)\} + \frac{n_y N}{2}\ln(2\pi) \quad \ldots(5)$$

where E_i denotes the residual error, expressed as $E_i = [Z(i) - Y(i)]$.

https://doi.org/10.1017/aer.2020.95 Published online by Cambridge University Press

In the optimisation procedure, it is assumed that the input data samples are well generated using the aerodynamic parameters and a priori measured motion and control variables for prediction of the observations. Hence, the measurement noise covariance matrix is known before the optimisation, which can be expressed as Equation (6) by applying the partial derivative of the cost function, $J\ (\Theta, R)$ w.r.t R:

$$R = \frac{1}{N}\sum_{i=1}^{N} E_i E_i^T \quad \ldots (6)$$

The cost function $J(\Theta)$ can thus be expressed as

$$J(\Theta) = \frac{1}{2} n_y N + \frac{N}{2} \ln\{\det(R)\} + \frac{n_y N}{2} \ln(2\pi) \quad \ldots (7)$$

The equation (7) includes constant terms, so without affecting the minimum value, the cost function, $J(\Theta)$ can be written in the simplest form as follows:

$$J(\Theta) = \det(R) \quad \ldots (8)$$

For optimisation of the unknown parameter vector Θ, the cost function, $J(\Theta)$ is minimised by applying the GN method and the parameter update vector, $\Delta\Theta$ in the k^{th} iteration is expressed as

$$\Delta\Theta = -\left[\left(\frac{\partial^2 J}{\partial \Theta^2}\right)_k\right]^{-1}\left(\frac{\partial J}{\partial \Theta}\right)_k \quad \ldots (9)$$

where the gradient vector, $\left(\frac{\partial J}{\partial \Theta}\right)$ of the k^{th} iteration is given as $\left(\frac{\partial J}{\partial \Theta}\right)_k = -\sum_{i=1}^{N}\left[\frac{\partial Y(i)}{\partial \Theta}\right]^T R^{-1} E_i$; the information matrix, $\left(\frac{\partial^2 J}{\partial \Theta^2}\right)$ of the k^{th} iteration is given as $\left(\frac{\partial^2 J}{\partial \Theta^2}\right)_k = \sum_{i=1}^{N}\left[\frac{\partial Y(i)}{\partial \Theta}\right]^T R^{-1}\left[\frac{\partial Y(i)}{\partial \Theta}\right]$, which is also known as the Hessian matrix. The response gradient matrix, $\left(\partial Y(i)/\partial\Theta\right)$ is computed by applying forward difference approximation theory.

The parameter vector of the $(k+1)^{\text{th}}$ iteration, Θ_{k+1} is computed by using the parameter vector of the k^{th} iteration, Θ_k as follows:

$$\Theta_{k+1} = \Theta_k + \Delta\Theta \quad \ldots (10)$$

3.2 Recurrent extreme learning machine-based parameter optimisation

The aircraft's motion is governed by the external forces and moments due to the aerodynamic effects, engine thrust and gravity, which is represented appropriately by the motion variables such as the true velocity of the aircraft, angle-of-attack, side-slip angle, attitude angles, angular rates, linear accelerations etc., and the control variables using the elevator, aileron and rudder deflections and the engine throttle setting. Such a concept has been applied previously in time-series neural modelling and parameter estimation for longitudinal and lateral directional motions[33,45,46]. The current research paper investigates the use of a recurrent neural model in the optimisation of the aerodynamic and stall parameters of the quasi-steady stall manoeuvre of an aircraft. Such a stall phenomenon is categorised as a large-amplitude

https://doi.org/10.1017/aer.2020.95 Published online by Cambridge University Press

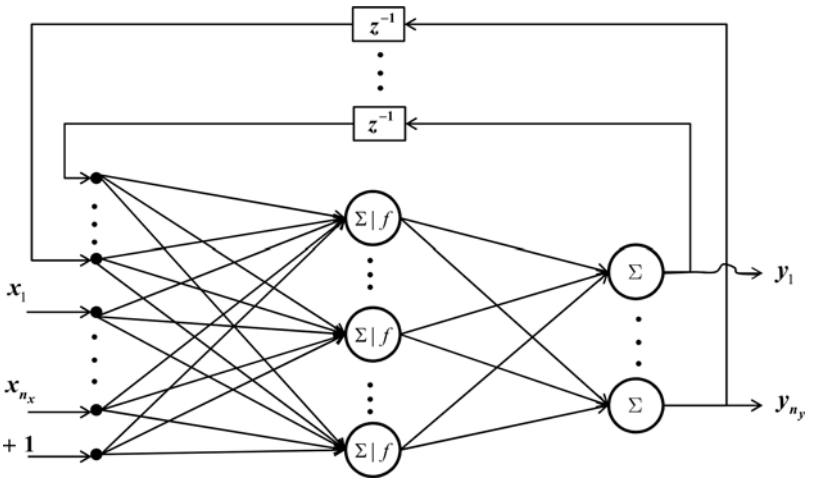


Figure 1. Structure of a typical recurrent neural model.

manoeuvre that exhibits hysteresis in the aerodynamic forces and moments with a considerable amount of turbulence near stall. In the present study, an RELM network is used for the nonlinear mapping between the input and output variables of dimension $X \in R^{n_x}$ and $Y \in R^{n_y}$, respectively. The network consists of a FFNN with feedback connections from the output nodes, adopting the structure of a conventional Jordan artificial neural network (ANN) as shown in Fig. 1. Let us assume a single hidden layer with neurons of dimension $H \in R^{n_h}$. In general, the output of such a network can be expressed mathematically using the time delays m and n in the input and output variables, respectively, as follows:

$$y(i+1) = f(x(i), ..., x(i-m), y(i), ..., y(i-n)) \quad \ldots (11)$$

The main objective of the present investigation is to use this network to optimise the aerodynamic parameters, hence the time delays in the input and output variables are restricted so as to avoid overfitting of the network. Most commonly, ANNs are trained using back-propagation algorithms such as steepest descent, Levenberg–Marquardt and scaled conjugate gradients, or using global optimisation algorithms such as the genetic algorithm, particle swarm optimisation, artificial bee colony optimisation etc., which may lead to overfitting and also may consume more time in some cases. Such issues are overcome by using the nonlinear mapping suggested by Huang et al. for a single hidden layer neural network, known as an ELM network[38–40]. The learning procedure for an ELM network is employed in the present study. The input variables of the network are considered to be the coefficients of the aerodynamic forces and moments (C_D, C_L, C_m) of the i^{th} instant, which are derived from the measured and geometric quantities of the aircraft as follows:

$$C_D(i) = -C_X(i)\cos(\alpha(i)) - C_Z(i)\sin(\alpha(i)) \quad \ldots (12)$$

$$C_L(i) = C_X(i)\sin(\alpha(i)) - C_Z(i)\cos(\alpha(i)) \quad \ldots (13)$$

$$C_m(i) = [I_y\dot{q}(i) + (p^2(i) - r^2(i))I_{xz} - p(i)r(i)(I_z - I_x) - T(i)z_{ENCG}]/(\bar{q}(i)S\bar{c}) \quad \ldots (14)$$

https://doi.org/10.1017/aer.2020.95 Published online by Cambridge University Press

where C_X, C_z are the body force coefficients, expressed as follows:

$$\begin{aligned} C_X(i) &= ma_X(i)/\bar{q}S \\ C_Z(i) &= ma_Z(i)/\bar{q}S \end{aligned} \quad \ldots(15)$$

In the supervised learning of the RELM network, the motion variables $(\alpha, \theta, q, V, a_x, a_z)$ are considered as $(i+1)^{\text{th}}$ instant target variables, while for their feedback to the input nodes, they are considered at the i^{th} instant. The input–output variables have different physical significance, hence their normalisation is essential to enhance the nonlinear mapping for a given flight dataset. Generally, the input and output variables are normalised within a specified range of $(\bar{x}_{\max}, \bar{x}_{\min})$ as follows[42]:

$$\bar{x}_i = \bar{x}_{i,\min} + \frac{(\bar{x}_{i,\max} - \bar{x}_{i,\min})}{(x_{i,\max} - x_{i,\min})}(x_i - x_{i,\min}) \quad \ldots(16)$$

In the supervised learning of the network, the input and output samples of the i^{th} instant are processed from the context nodes to the neurons of the hidden layer through the connecting elements of the input weight matrix, $\bar{V}$ with dimension $(n_x + n_y + 1) \times n_h$. Log sigmoid-based transfer functions are used in the neurons of the hidden layer, thus the output of the j^{th} neuron is given by the expression

$$\bar{h}_j = g\left(\sum_{i=1}^{n_x} \bar{x}_i \bar{v}_{ij} + \sum_{i=n_x+1}^{n_y} \bar{y}_i \bar{v}_{ij} + \bar{v}_{(n_x+n_y+1)j}\right) \quad \ldots(17)$$

where $i = 1, 2, 3, ..., (n_x + n_y + 1)$; $j = 1, 2, 3, ..., n_y$; $\bar{v}_{ij}$ denotes the connecting element of $\bar{V}$ between the i^{th} and j^{th} neuron of the input and hidden layer, respectively; $\bar{v}_{(n_x+n_y+1)j}$ denotes the bias of the j^{th} neuron of the hidden layer; $g(\cdot)$ denotes the transfer function relationship of the log sigmoid used by the hidden layer neuron.

Let us assume that the weight between the hidden and output layer is $\bar{W}$. Therefore, the k^{th} node of the network's output layer can be approximated using the elements of the output weight, $\bar{W}$ as follows:

$$\bar{y}_k = \sum_{j=1}^{n_h} \bar{h}_j \bar{w}_{jk} \quad \ldots(18)$$

where $k = 1, 2, 3, ..., n_y$; $\bar{h}_j$ denotes the output of the j^{th} neuron of the hidden layer; $\bar{w}_{jk}$ denotes the element of the output weight $\bar{W}$ between the j^{th} neuron and the k^{th} node of the hidden and output layer, respectively.

Equations (17) and (18) represent a typical way of processing the data through a single hidden layer recurrent neural model. The output of the hidden layer neurons can be expressed in vector form as $\bar{H} = [\bar{h}_1\ \bar{h}_2\ \cdots\ \bar{h}_{n_h}]$, thus the predicted output can be given as $\bar{Y} = \bar{H}\bar{W}$. In the supervised learning of the network, the objective is to minimise the residual error between the predicted and measured output for output weight $\bar{W}$ as follows:

$$\min_{\bar{W}} \ ||\bar{H}\bar{W} - \bar{Z}|| \quad \ldots(19)$$

https://doi.org/10.1017/aer.2020.95 Published online by Cambridge University Press

Equation (19) becomes a set of linear equations $\bar{H}\bar{W} = \bar{Z}$ that provides a number of solutions. Huang et al.[38–40] suggested to use the minimum norm of $\bar{W}$ among all the solutions. The output weight can be estimated as follows:

$$\bar{H}\bar{W} = \bar{Z} \;\rightarrow\; \hat{\bar{W}} = \bar{H}^{\dagger}\bar{Z} \qquad \ldots(20)$$

where $\bar{H}^{\dagger} = \left(\bar{H}^{T}\bar{H}\right)^{-1}\bar{H}^{T}$ is a Moore–Penrose generalised inverse matrix of $\bar{H}$. The equation (20) can be determined analytically for given input weights, biases and number of hidden layer neurons. Bartlett[41] pointed out that the magnitude of the network weights is more important than the value of the residual error of the training example in terms of performance generalisation. A smaller norm of the network weight would tend to indicate better generalisation. As analysed above, the learning procedure not only reaches a smaller value of the residual error but also a smaller norm of the output weight for given input weights and hidden layer neuron biases.

In this study, we use two statistical measures, namely the mean square error (MSE) and the coefficient of determination (R^2), to describe the training and generalisation abilities of the RELM network[43,46]. The MSE is defined as the mean of the sum of the squared error between the predicted and measured quantities and is expressed as follows:

$$MSE = \frac{1}{n_y N}\sum_{i=1}^{N}(Y_i - Z_i)^2 \qquad \ldots(21)$$

The coefficient of determination (R^2) is a quantity used to assess the quality of the prediction by the neural model by illustrating how well the nonlinear map operates between the chosen input–output dataset. The value of R^2 lies between 0.0 and 1.0. A value closer to 1.0 indicates good predictions for similar input data samples. It is expressed for the chosen network as follows:

$$R^2 = \frac{1}{n_y}\left[1 - \frac{\sum_{i=1}^{N}(Z_i - Y_i)^2}{\sum_{i=1}^{N}(Z_i - Z_{avg.})^2}\right] \qquad \ldots(22)$$

where $Z_{avg.}$ denotes the mean of the measured output data samples, Z.

This optimisation methodology is applied herein to extract the aerodynamic parameters of a postulated aerodynamic model using the RELM network as shown in Fig. 2. The structure of the recurrent neural model is used for predictions of similar input samples. The input variables of the neural model are the coefficients of the aerodynamic forces and moment, which are computed in two ways. The first approach employs the computation based on the measurements of the linear and angular accelerations as expressed in Equations (12)–(14), as utilised in the training of the neural model. The other approach is to postulate them by applying Taylor's series expansion theory on the governing functions of the coefficients with respect to the motion and control variables measured during flight. The latter approach is commonly used in the postulation of aerodynamic models and can be computed analytically for given values of the parameters. In solving the parameter identification problem, one must optimise the parameters of the aerodynamic model using some optimisation algorithm based on the residual error minimisation principle.

https://doi.org/10.1017/aer.2020.95 Published online by Cambridge University Press

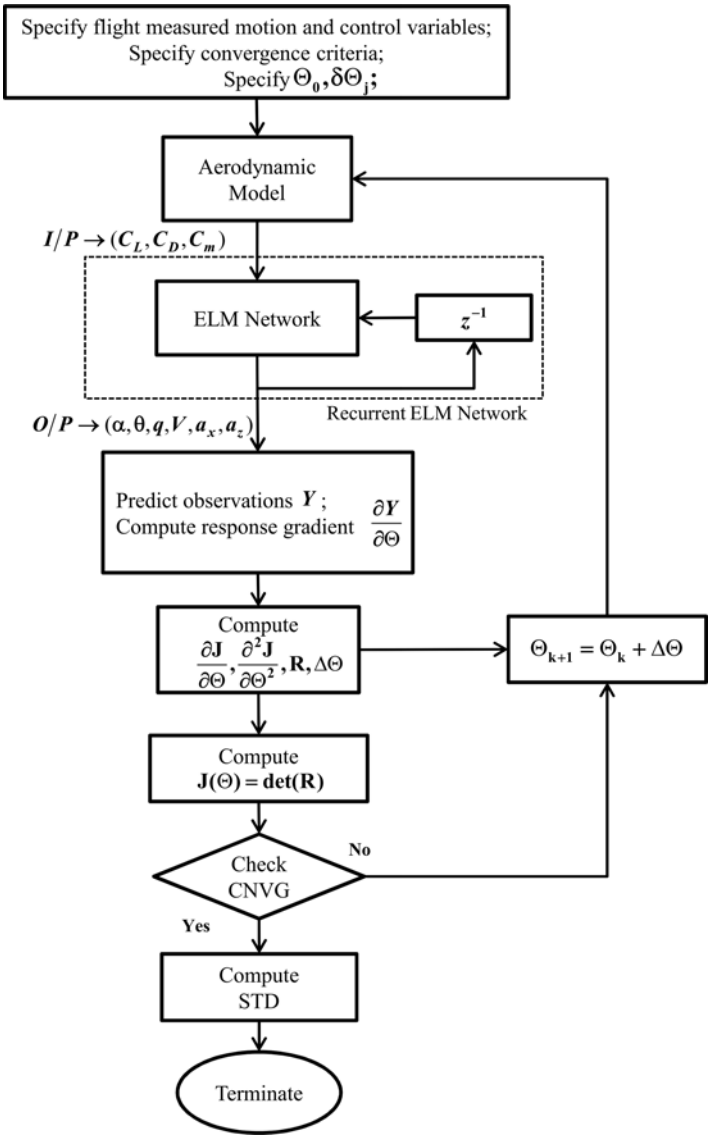


Figure 2. Flow chart of the RELM-GN optimisation methodology.

In the optimisation of the stability and control derivatives, denoted as Θ, the observations are predicted by propagating the analytically generated input samples through the RELM network as follows:

$$Y(i+1) = f(X(i), Y(i), \bar{V}, \bar{W}, \Theta) \quad \ldots (23)$$

where $f(\bullet)$ denotes the nonlinear function relationship of the RELM network; $Y(i+1)$ is a vector of the predicted observations of the $(i+1)^{\text{th}}$ instant; $Y(i)$ is a vector of the training observations of the i^{th} instant; $X(i)$ is a vector of the input samples of the i^{th} instant; $\bar{V}, \bar{W}$ are the input and output weight matrix, respectively.

https://doi.org/10.1017/aer.2020.95 Published online by Cambridge University Press

The coefficients of the aerodynamic forces and moment are computed analytically using the initial parameters (Θ_0), and the generated input samples are propagated through the trained RELM network to obtain their corresponding predictions using Equation (23). Similarly, the response gradient matrix $\left(\partial Y(i)/\partial\Theta\right)_{ij}$ is computed for each of the perturbed parameters $(\Theta + \delta\Theta_j)$ by applying the forward difference approximation theory as follows:

$$\left(\frac{\partial Y(i)}{\partial \Theta}\right)_{ij} \approx \frac{f\left(X\left(i-1\right), Y\left(i-1\right), \bar{V}, \bar{W}, \left(\Theta + \delta\Theta_j\right)\right) - f\left(X\left(i-1\right), Y\left(i-1\right), \bar{V}, \bar{W}, \Theta\right)}{\delta\Theta_j} \quad \ldots(24)$$

where $i = 1, 2, 3, ..., N$; $j = 1, 2, 3, ..., n_\Theta$; $\delta\Theta_j$ denotes a small perturbation in the j^{th} parameter of Θ.

Furthermore, the cost function is computed by using Equation (8), and the convergence (CNVG) of the algorithm is checked. If the optimisation process does not converge, then the parameters are updated by following Equations (9) and (10) of the GN method. The optimisation process is continued until convergence occurs.

Finally, the statistical value of the optimised parameter in terms of the standard deviation (STD) is computed, given by the square root of the diagonal element of the estimation error covariance matrix, P, as follows:

$$\sigma_{\Theta_j} = \sqrt{p_{jj}} \quad \ldots(25)$$

where $j = 1, 2, 3, ..., n_\Theta$; P is approximated as the inverse of the Hessian matrix as follows:

$$P \approx \left\{\sum_{i=1}^{N}\left[\frac{\partial Y(i)}{\partial \Theta}\right]^T\left[R^{-1}\right]\left[\frac{\partial Y(i)}{\partial \Theta}\right]\right\}^{-1} \quad \ldots(26)$$

3.3 Model validation

Generally, the model is validated by the quality of fit using one of the statistical approaches. Theil's inequality coefficient (TIC) is one of these, being used to represent the goodness of fit in terms of the residuals[2] and expressed as

$$U = \frac{\sqrt{\frac{1}{N}\sum_{i=1}^{N}\left[z_i - y_i\right]^2}}{\sqrt{\frac{1}{N}\sum_{i=1}^{N} z_i^2} + \sqrt{\frac{1}{N}\sum_{i=1}^{N} y_i^2}} \quad \ldots(27)$$

where z and y are the measured and model predicted responses, respectively. U is a normalised index whose value lies in the range [0, 1]. $U = 0$ corresponds to the case of equality, whereas $U = 1$ corresponds to the case of maximum inequality.

4.0 RESULTS AND DISCUSSION

In this section, the efficacy of the recurrent ELM network-based optimisation methodology is demonstrated for the estimation of the aerodynamic parameters from real flight data of the ATTAS research aircraft. Two sets of real flight data from the aircraft are considered for

https://doi.org/10.1017/aer.2020.95 Published online by Cambridge University Press

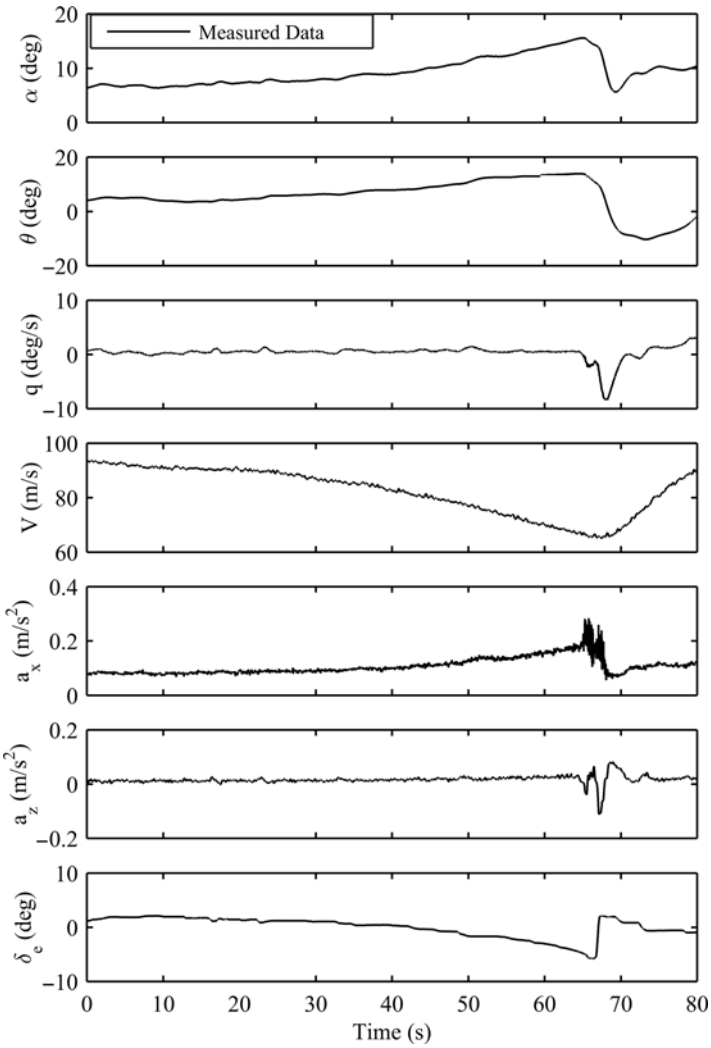


Figure 3. QSSM flight data of the ATTAS aircraft: RFD01.

estimating the parameters of the aerodynamic model, being gathered at an altitude of 16,000ft with the aircraft undergoing a quasi-steady stall manoeuvre. The manoeuvre is excited by commanding the elevator such that the rate of change of the angle-of-attack is nearly zero until stall takes place. Later, the elevator command is returned to the trim condition and the engine thrust is increased to compensate for the loss of velocity to bring the aircraft back from the stall state[2]. The raw flight data are subject to a compatibility check to improve its quality, and the corrected flight data shown in Figs 3 and 4 are applied in the present study.

The unknown parameters, namely $C_{D0}, e, C_{L0}, C_{L\alpha}, C_{L\alpha Ma}, C_{m0}, C_{m\alpha}, C_{mq}, C_{m\delta e}, a_1, \alpha^*, \tau_2$, $\partial C_D/\partial\chi, \partial C_m/\partial\chi$, of the postulated aerodynamic model are to be determined using the parameter estimation methods. The control derivative $C_{L\delta e}$ is computed directly from the moment derivative using the expression $-C_{m\delta e}\bar{c}/r_h$. A flight dynamic neural model is generated using the RELM network according to the previous section, where the values of MSE and R^2 are found to be 4.49E–02, 0.9932 with RFD01 and 5.29E–02, 0.9930 with RFD02,

https://doi.org/10.1017/aer.2020.95 Published online by Cambridge University Press

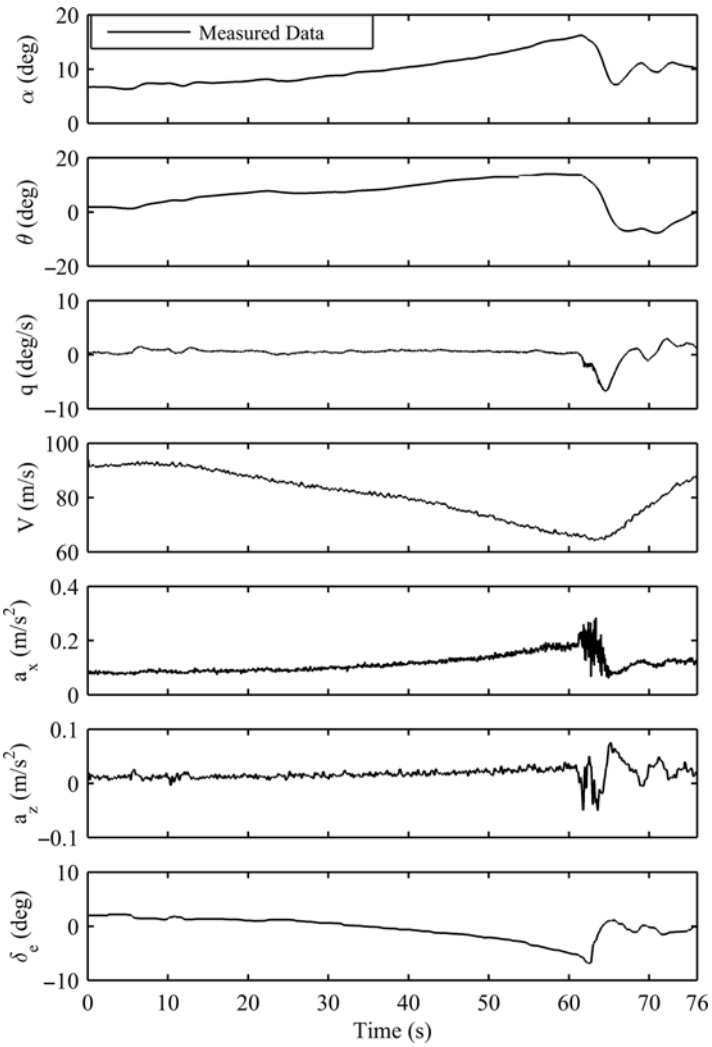


Figure 4. QSSM flight data of the ATTAS aircraft: RFD02.

respectively. It is observed that these values confirm the qualitative generalisation between the chosen input and output variables of the network for the investigation of the unknown parameters using the suggested RELM-GN estimation procedure. The predicted quantities match satisfactorily with their corresponding measured values in spite of the significant amount of noise present in the linear accelerations. Further, the GN optimisation method is applied to compute the aerodynamic and stall parameters with the propagation of the generated input data using the coefficients of forces and moment, and the optimal estimates are presented with their corresponding standard deviations in Table 1. To validate the RELM-GN estimates, the MLE method is applied to estimate the same parameters from the real flight data without considering the integration of the aircrafts' dynamic equations as the conventional parameter estimation methods pose difficulty[2,20,47].

In Table 1, the RELM-GN estimates of the lift and drag forces are in good agreement with the estimates obtained using the MLE method, with lower values of their respective standard

https://doi.org/10.1017/aer.2020.95 Published online by Cambridge University Press

Table 1
Longitudinal Estimates of ATTAS Aircraft: QSSM

	RFD01		RFD02	
$\hat{\Theta}$	MLE	RELM-GN	MLE	RELM-GN
C_{L_0}	0.1927	0.1973	0.1759	0.1835
	(0.0047)	(0.0037)	(0.0057)	(0.0043)
C_{L_α}	3.8053	3.9384	3.8914	3.9066
	(0.0477)	(0.0412)	(0.0502)	(0.0396)
$C_{L_{\alpha Ma}}$	5.8391	5.2561	6.0334	5.8086
	(0.2620)	(0.2049)	(0.2969)	(0.2195)
C_{D_0}	0.0404	0.0417	0.0411	0.0417
	(0.0007)	(0.0006)	(0.0008)	(0.0006)
e	0.7818	0.8067	0.7882	0.7949
	(0.0090)	(0.0086)	(0.0089)	(0.0075)
C_{m_0}	0.1208	0.1106	0.1361	0.1147
	(0.0027)	(0.0044)	(0.0029)	(0.0045)
C_{m_α}	−0.6085	−0.5314	−0.6991	−0.5663
	(0.0166)	(0.0280)	(0.0178)	(0.0278)
C_{m_q}	−16.6308	−20.0428	−14.9243	−16.2061
	(0.4254)	(0.6771)	(0.4031)	(0.6965)
$C_{m_{\delta e}}$	−1.1185	−1.0392	−1.2329	−1.0285
	(0.0225)	(0.0363)	(0.0254)	(0.0390)
a_1	32.0452	27.0035	33.2809	29.3869
	(1.2785)	(1.3166)	(0.8723)	(1.0297)
α^*	0.3111	0.3141	0.3111	0.3103
	(0.0021)	(0.0023)	(0.0010)	(0.0011)
τ_2	33.4986	34.2172	43.9138	40.6499
	(0.4471)	(0.6189)	(0.4925)	(0.6359)
$\partial C_D / \partial \chi$	0.2546	0.2116	0.1032	0.1033
	(0.0237)	(0.0174)	(0.0080)	(0.0082)
$\partial C_m / \partial \chi$	−0.5600	−0.4997	−0.3328	−0.3072
	(0.0440)	(0.0356)	(0.0129)	(0.0140)

Note: Values in parenthesis denote standard deviations.

deviations. The value of C_{L_α} varies approximately from 3.8 to 3.9, whereas the values of C_{D_0} and the Oswald factor, e, are approximately 0.04, and 0.8, respectively, in the estimations using both datasets. Among the pitching moment derivatives, the values of $C_{m_0}, C_{m_\alpha}, C_{m_{\delta e}}$ estimated using RELM-GN are found to be closer to the MLE values, whereas a variation is observed in the values of C_{m_q}. The value of α^* is approximately 0.31rad ($\approx$17.7 deg) from both datasets, demonstrating the consistency in the estimations. However, the values of the other stall parameters a_1 and τ_2 are observed to be closer in their respective flight dataset analysis. The additional drag due to the unsteady aerodynamics is obtained from the estimate

https://doi.org/10.1017/aer.2020.95 Published online by Cambridge University Press

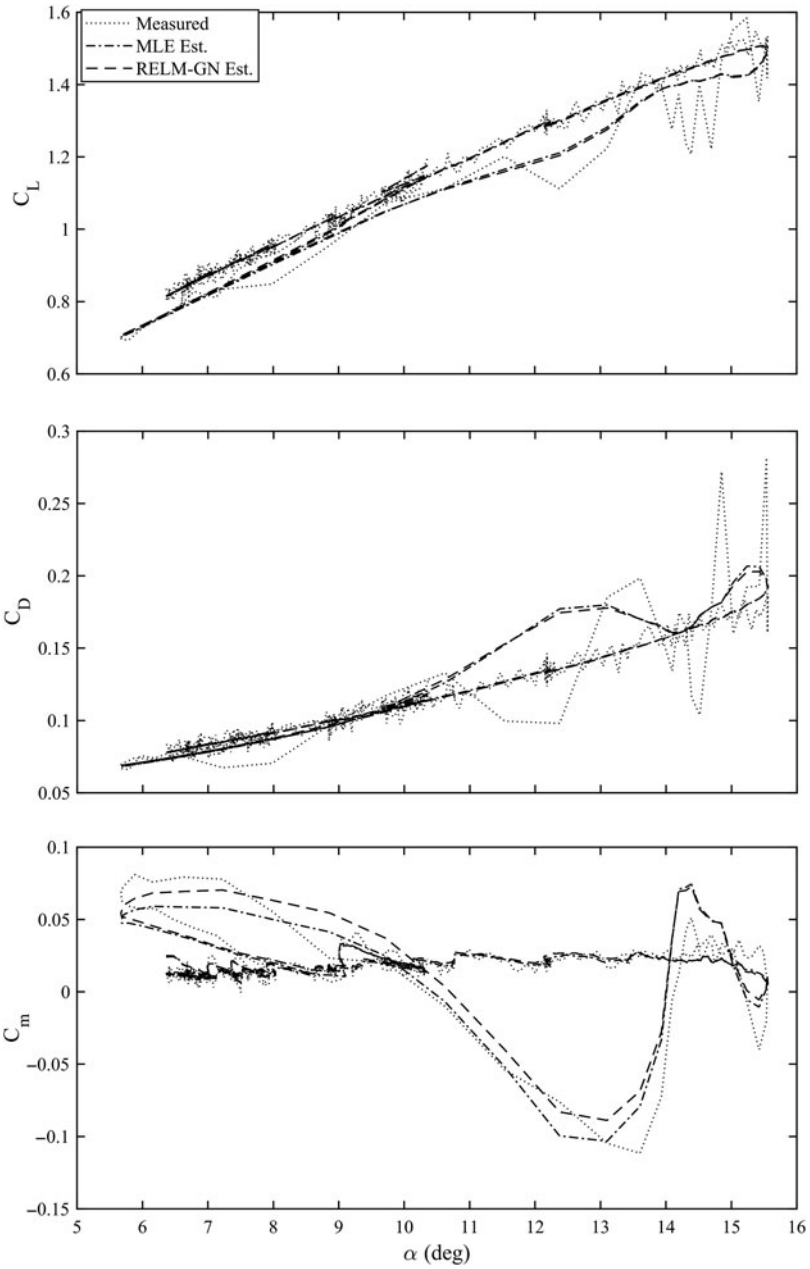


Figure 5. Estimated C_L, C_D, C_m versus α: RFD01.

of $\partial C_D / \partial \chi$, whose value is promising from both flight datasets, although the major contribution to the unsteady drag is obtained from the lift contribution due to the flow separation. The value of $\partial C_m / \partial \chi$, which models the hysteresis effect in the pitching moment, is also found within the bounds, although the values obtained from both flight datasets differ in magnitude due to the variations in the post-stall unsteady effects. Figures 5 and 6 present a comparison of the measured and estimated lift, drag and pitching moment coefficients versus the

https://doi.org/10.1017/aer.2020.95 Published online by Cambridge University Press

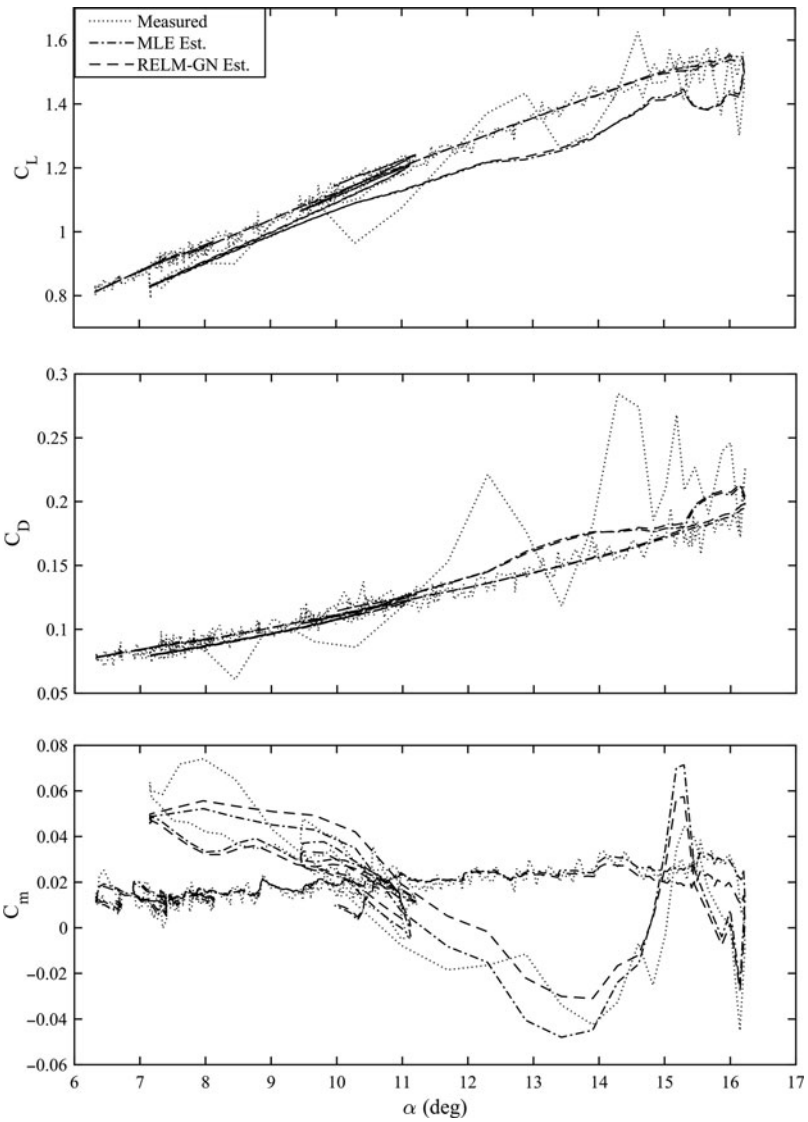


Figure 6. Estimated C_L, C_D, C_m versus α: RFD02.

angle-of-attack for RFD01 and RFD02, respectively. It is observed that the estimated values of the slopes $C_{L\alpha}, C_{D\alpha}, C_{m\alpha}$ match satisfactorily with their respective measured value up to the stall angles, whereas some variations are observed in the post-stall region due to the unsteady effects. Further, it can also be concluded that the obtained estimates are reliable in the presence of noise resulting from buffeting.

Further, the capability of the aerodynamic model is confirmed by the proof-of-match exercise when comparing the model-predicted aerodynamic forces and moment coefficients with their respective measured coefficients in Fig. 7. The simulation is carried out using the elevator command of RFD01 and the estimates obtained using the MLE and RELM-GN methods applied to the flight dataset RFD02. Theil's inequality coefficient is also computed for the

https://doi.org/10.1017/aer.2020.95 Published online by Cambridge University Press

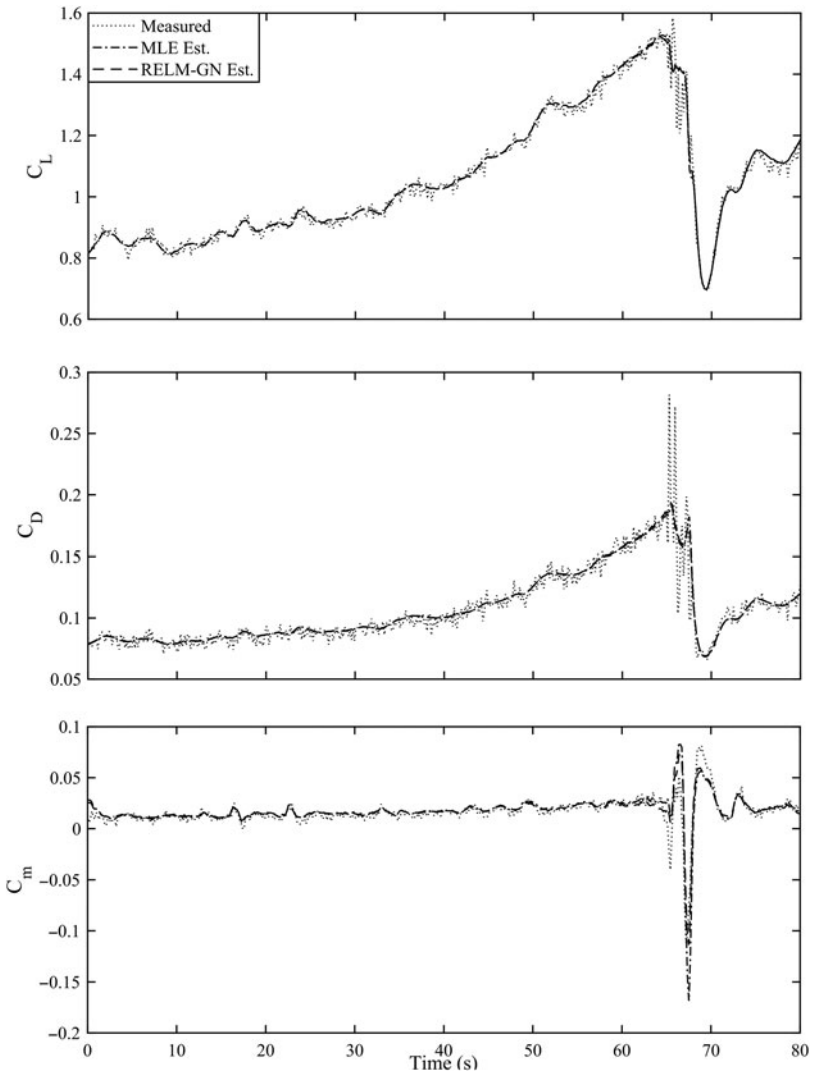


Figure 7. Comparison of simulated and measured C_L, C_D, C_m.

overall fitting between the model predicted and measured responses. The TIC values for the estimated C_L, C_D, C_m are 0.0140, 0.0446, 0.2105 using the estimates obtained by the MLE method and 0.0135, 0.0438, 0.1687 when using the RELM-GN algorithm, respectively. It is observed that the TIC values using the estimates of RELM-GN algorithm are found to be relatively smaller than those obtained when using MLE method. It can also be observed from Fig. 7 that the estimated C_L, C_D, C_m have been fitted satisfactorily with the corresponding measured coefficients in the presence of turbulence near the stall region.

5.0 CONCLUSION

A recurrent ELM network is studied to show the efficacy of such neural modelling for the estimation of the aerodynamic and stall parameters from two real flight datasets during a QSSM.

https://doi.org/10.1017/aer.2020.95 Published online by Cambridge University Press

The network parameters are chosen appropriately based on the variables of the input–output space, number of samples and noise content of the data to achieve a lower MSE and higher R^2 for better generalisation capability of the network in the predictions. It is found that the network may lead to under- or over-fitting for a smaller or greater number of hidden layer neurons, respectively, which demonstrates the incapability of the network in the prediction as well as the estimation. The statistical values of MSE and R^2 obtained from the neural modelling indicate a satisfactory nonlinear mapping with the chosen flight dataset for the longitudinal motion, which also confirms the qualitative generalisability of the network for use in parameter optimisation based on the RELM-GN algorithm. It is found that the estimates of the proposed algorithm are reliable in comparison with those of MLE method, and furthermore, the validation against the simulated responses illustrates the capability of the proposed algorithm in the presence of noise. Moreover, the proposed algorithm is found to be effective for qualitative estimation of nonlinear aerodynamic model parameters, where conventional parameter estimation methods face difficulty due to the unsteady aerodynamics during a QSSM. It is observed that mathematical modelling of aircraft dynamics is a difficult task without inclusion of the cross-coupling effect near stall. This issue can be efficiently addressed by using the proposed RELM-GN algorithm without inclusion of the lateral directional motion and control variables, or the need to integrate the equations of motion of the aircraft. In addition, the proposed algorithm has also been verified for parameter estimation of the postulated linear aerodynamic models at moderate angles of attack. Therefore, the RELM-GN algorithm could be a better choice for dynamic modelling and parameter estimation in stall and post-stall regions, where the mathematical description of the system dynamics is difficult and lower computational cost is required.

REFERENCES

1. HAMEL, P.G. and JATEGAONKAR, R.V. Evolution of flight vehicle system identification, *J Aircr* 1996, **33**, (1), pp 9–28. doi: 10.2514/3.46898
2. JATEGAONKAR, R.V. *Flight Vehicle System Identification: A Time Domain Methodology*; 1st ed., vol. **216**, Progress in Astronautics and Aeronautics, AIAA, 2006, Reston, VA. doi: 10.2514/4.866852
3. RAOL, R, JITENDRA, G.G. and SINGH, J. *Modelling and Parameter Estimation of Dynamic System*, IET, 2004, London, UK.
4. PAMADI, B.N. *Performance, Stability, Dynamics and Control of Airplanes*, AIAA Education Series, 1998, Virginia.
5. FILIPPONE, A. *Flight Performance of Fixed and Rotary Wing Aircraft*, Elsevier, 2006, Oxford, UK.
6. GHOREYSHI, M. and CUMMINGS, R.M. Challenges in the aerodynamics modeling of an oscillating and translating airfoil at large incidence angles, *J Aerosp Sci Technol* 2013, **28**, (1), pp 176–190. doi: 10.1016/j.ast.2012.10.013.
7. KYLE, H., LOWENBERG, M. and GREENWELL, D. Comparative evaluation of unsteady aerodynamic modeling approaches, *AIAA Paper 2004-5272*, August 2004. doi: 10.2514/6.2004-5272
8. GREENWELL, D. A review of unsteady aerodynamic modeling for flight dynamics of manoeuvrable aircraft. *AIAA Paper 2004-5276*; August 2004. doi: 10.2514/6.2004-5276
9. RONCH, A.D., BADCOCK, K.J., GHOREYSHI, M. and CUMMINGS, R.M. Modeling of unsteady aerodynamic loads, *AIAA Paper 2011-6524*, August 2011. doi: 10.2514/6.2011-6524
10. TOBAK, M. and SCHIFF, L.B. On the formulation of the aerodynamic characteristics in aircraft dynamic, NASA TR R-456, Washington, DC, 1976.
11. REISENTHEL, P.H. and BETTENCOURT, M.T. Data-based aerodynamic modeling using nonlinear indicial theory, *AIAA Paper 99-0763*, January 1999. doi: 10.2514/6.1999-763
12. GHORYESHI, M., JIRÁSEK, A. and CUMMINGS, R.M. Computational investigation into the use of response functions for aerodynamic loads modeling, *AIAA J*, 2012, **50**, (6), pp 1314–1327. doi: 10.2514/1.J051428

https://doi.org/10.1017/aer.2020.95 Published online by Cambridge University Press

13. GHOREYSHI, M. and CUMMINGS, R.M. Unsteady aerodynamics modeling for aircraft maneuvers: a new approach using time-dependent surrogate modeling, *J Aerosp Sci Technol* 2014, **39**, pp 222–242. doi: 10.1016/j.ast.2014.09.009
14. LEISHMAN, J.G. and NGUYEN, K.Q. State space representation of unsteady airfoil behavior, *AIAA J* 1990, **28**, (5), pp 836–844. doi: 10.2514/3.25127
15. GOMAN, M.G. and KHRABROV, A.N. State-space representation of aerodynamic characteristics of an aircraft at high angles of attack, *J Aircr* 1994, **31**, (5), pp 1109–1115. doi: 10.2514/3.46618
16. FISCHENBERG, D. Identification of an unsteady aerodynamic stall model from flight test data, *AIAA Paper 1995-3438*, 1995. doi: 10.2514/6.1995-3438
17. FISCHENBERG, D. and JATEGAONKAR, R.V. Identification of aircraft stall behavior from flight test data. *RTO MP-11 Paper No. 17*, 1999.
18. MAINE, R.E. and ILIFF, K.W. Application of parameter estimation to aircraft stability and control – the output-error approach. *NASA RP 1168*, January 1986.
19. MORELLI, E.A. and KLEIN, V. Application of system identification to aircraft at NASA Langley Research Center, *J Aircraft*, 2005, **42**, (1), pp 12–25. doi: 10.2514/1.3648
20. JATEGAONKAR, R.V. and PLAETSCHKE, E. Identification of moderately nonlinear flight mechanics systems with additive process and measurement noise, *J Guidance Cont Dyn*, 1990, **13**, (2), pp 277–285. doi: 10.2514/3.20547
21. KAMALI, C., PASHILKAR, A.A. and RAOL, J.R. Evaluation of recursive least squares algorithm for parameter estimation in aircraft real time applications, *J Aerospace Science and Technology* 2011, **15**, (3), pp 165–174. doi: 10.1016/j.ast.2010.12.007
22. CHOWDHARY, G. and JATEGAONKAR, R.V. Aerodynamic parameter estimation from flight data applying extended and unscented Kalman filter, *J Aerospace Science and Technology* 2010, **14**, (2), pp 106–117. doi: 10.1016/j.ast.2009.10.003
23. SEO, G., KIM, Y. and SADERLA, S. Kalman-filter based online system identification of fixed-wing aircraft in upset condition, *J Aerosp Sci Technol* 2019, **89**, pp 307–317. doi: 10.1016/j.ast.2019.04.012
24. IGNATYEV, D., KHRABROV, A. and ALEXANDER, N. Neural network modeling of unsteady aerodynamic characteristics at high angles of attack, *J Aerosp Sci Technol* 2015, **41**, pp 106–115. doi: 10.1016/j.ast.2014.12.017
25. LYU, Y., ZHANG, W., SHI, J., QU, X. and CAO, Y. Unsteady aerodynamic modeling of biaxial coupled oscillation based on improved ELM, *J Aerosp Sci Technol* 2017, **60**, pp 58–67. doi: 10.1016/j.ast.2016.10.029
26. WANG, Q., QIAN, W. and HE, K., Unsteady aerodynamic modelling at high angles of attack using support vector machines, *Chin J Aeronaut*, 2015, **28**, (3), pp 659–668. doi: 10.1016/j.cja.2015.03.010
27. KUMAR, A. and GHOSH, A.K., Decision tree and random forest based novel unsteady aerodynamics modeling using flight data, *J Aircr* 2019, **56**, (1), pp 403–409. doi: 10.2514/1.C035034
28. LINSE, D.J. and STENGEL, R. Identification of aerodynamic coefficients using computational neural networks, *J Guidance Cont Dyn* 1993, **16**, (6), pp 1018–1025. doi: 10.2514/3.21122
29. RAOL, J.R. and JATEGAONKAR, R.V. Aircraft parameter estimation using recurrent neural networks – a critical appraisal, *AIAA Paper* 95-3504, 1995. doi: 10.2514/6.1995-3504
30. RAISINGHANI, S.C., GHOSH, A.K. and KALRA, P.K. Two new techniques for aircraft parameter estimation using neural networks, *Aeronautical J*, 1998, **102**, (1011), pp 25–30. doi: 10.1017/S0001924000065702
31. SINGH, S. and GHOSH, A.K. Estimation of lateral-directional parameters using neural network based modified delta method. *Aeronautical J*, 2007, **111**, (1124), pp 659–667. doi: 10.1017/S0001924000004838
32. SINHA, M., KUTTIERI, R.A., GHOSH, A.K. and MISRA, A. High angle of attack parameter estimation of cascaded fins using neural network, *J Aircraft*, 2013, **50**, (1), pp 272–291. doi: 10.2514/1.C031912
33. PEYADA, N.K. and GHOSH, A.K. Aircraft parameter estimation using new filtering technique based on neural network and gauss-newton method, *Aeronautical J*, 2009, **113**, (1,142), pp. 243–252. doi: 10.1017/S0001924000002918
34. KUMAR, R. and GHOSH, A.K. Nonlinear longitudinal aerodynamic modeling using neural gauss-newton method, *J Aircr*, 2011, **48**, (5), pp. 1809–1812. doi: 10.2514/1.C031253

https://doi.org/10.1017/aer.2020.95 Published online by Cambridge University Press

35. KUMAR, R., GHOSH, A.K. and MISRA, A. Parameter estimation from flight data of hansa-3 aircraft using quasi-steady stall modeling, *J Aerosp Eng*, 2013, **26**, (3), pp. 544–554. doi: 10.1061/(ASCE)AS.1943-5525.0000155
36. SADERLA, S., DHAYALAN, R. and GHOSH, A.K., Parameter estimation from near stall flight data using conventional and neural based methods, *Defence Sci J*, 2017, **67**, (1), pp 3–11. doi: 10.14429/dsj.67.9995
37. ROY, A.G. and PEYADA, N.K., Aircraft parameter estimation using hybrid neuro fuzzy and artificial bee colony optimization (HNFABC) algorithm, *J Aerosp Sci Technol*, 2017, **71**, pp. 772–782. doi: 10.1016/j.ast.2017.10.030
38. HUANG, G.B., ZHU, Q.Y. and SIEW, C.K. Extreme learning machine: A new learning scheme of feed forward neural networks, IEEE International Joint Conference on Neural Networks, 2004, Budapest, Hungary. doi: 10.1109/IJCNN.2004.1380068
39. HUANG, G.B., ZHU, Q.Y. and SIEW, C.K. Extreme learning machine: Theory and applications. *Neurocomputing* 2006, **70**, (1–3), pp 489–501. doi: 10.1016/j.neucom.2005.12.126
40. HUANG, G.B., ZHOU, H., DING, X. and ZHANG, R. Extreme learning machine for regression and multiclass classification, *IEEE Trans Syst Man Cybern*, 2012, **42**, (2), pp 513–529. doi: 10.1109/TSMCB.2011.2168604
41. BARTLETT, P.L., The sample complexity of pattern classification with neural networks: the size of the weights is more important than the size of the network, *IEEE Trans Inform Theory*, 1998, **44**, (2), pp. 525–536. doi: 10.1109/18.661502
42. SOLA, J. and SEVILLA, J., Importance of data normalization for the application of neural networks to complex industrial problems, *IEEE Trans Nuclear Sci*, 1997, **44**, (3), pp. 1464–1468. doi: 10.1109/23.589532
43. SAHIN, M. Comparison of modelling ANN and ELM to estimate solar radiation over Turkey using NOAA satellite data, *International JRemote Sensing*, 2013, **34**, (21), pp 7508–7533. doi: 10.1080/01431161.2013.822597
44. MALATHI, V., MARIMUTHU, N., BASKAR, S. and RAMAR, K. Application of extreme learning machine for series compensated transmission line protection, *Eng Appl Artif Intell*, 2011, **24**, (5), pp. 880–887. doi: 10.1016/j.engappai.2011.03.003.
45. VERMA, H.O. and PEYADA, N.K., Parameter estimation of stable and unstable aircraft using extreme learning machine, *AIAA 2018-0526*, 2018. doi: 10.2514/6.2018-0526
46. VERMA, H.O. and PEYADA, N.K., Parameter estimation of aircraft using extreme learning machine and Gauss-Newton algorithm, *Aeronautical J*, 2020, **124**, (1272), pp 271–295. doi: 10.1017/aer.2019.123
47. MORELLI, E.A., Practical aspects of the equation error method for aircraft parameter estimation, *AIAA Atmospheric Flight Mechanics Conference*, Keystone, Colorado, USA., 2006. doi: 10.2514/6.2006-6144

https://doi.org/10.1017/aer.2020.95 Published online by Cambridge University Press